Supplementary Materials

Accelerated Microwave-Assisted Synthesis and *In-Situ* X-ray Scattering of Tungsten-Substituted Vanadium Dioxide ($V_{1-x}W_xO_2$)

Catrina E. Wilson,[1,2,¶] Amanda E. Gibson,[1,2,¶] Joshua J. Argo,[1,2] Patricia A. Loughney,[1,2] Wenqian Xu,[3] Graham King,[4] and Vicky Doan-Nguyen[1,2,5,*]

[1]*Department of Materials Science and Engineering, The Ohio State University, Columbus, OH 43212*

[2] *Center for Electron Microscopy and Analysis, The Ohio State University, Columbus, OH 43212*

[3]*X-ray Science Division, Advanced Photon Source, Argonne National Laboratory, Lemont, IL 60439*

[4]*Brockhouse Beamlines, Canadian Light Source, Saskatoon, SK S7N 2V3 Canada*

[5] *Department of Mechanical and Aerospace Engineering, The Ohio State University, Columbus, OH 43210*

¶*Contributed equally to this work*

**Address all correspondence to this author. Email:* doan-nguyen.1@osu.edu

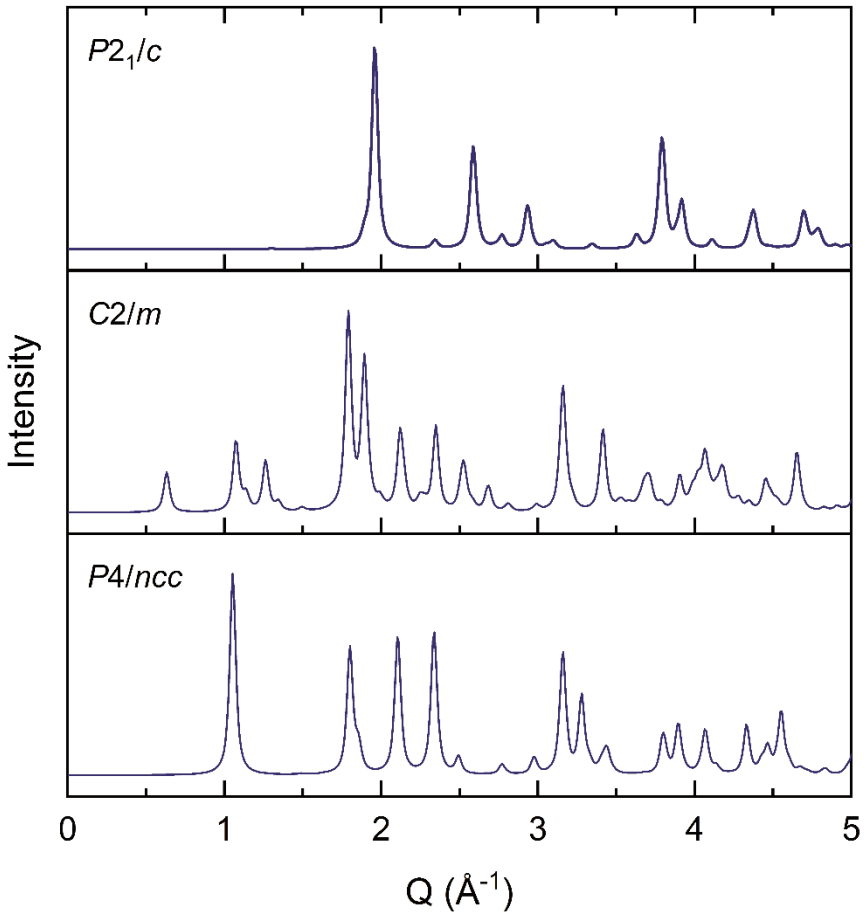

Figure S1: Simulated powder diffraction patterns for various VO_2 phases.

Table SI: Microwave-synthesized VO_2, *P2₁/c*, structural parameters:
a = 5.753(2) Å, *b* = 4.5253(1) Å, *c* = 5.382(2) Å, *b* = 122.604(3)°

Atom	Wyckoff Position	x	y	z	Occ.	U_{iso} (Å^2)
V	4e	0.2386(2)	0.9793(2)	0.0259(2)	1.0	0.0050(2)
O1	4e	0.1076(8)	0.2108(8)	0.2078(9)	1.0	0.0087(3)
O2	4e	0.4035(8)	0.7049(8)	0.3009(8)	1.0	0.0087(3)

Table SII: Microwave-synthesized $W_{0.003}V_{0.997}O_2$, *P2₁/c*, structural parameters:
a = 5.750(2) Å, *b* = 4.5260(1) Å, *c* = 5.380(2) Å, *b* = 122.577(4)°

Atom	Wyckoff Position	x	y	z	Occ.	U_{iso} (Å^2)
V	4e	0.2397(2)	0.9804(3)	0.0271(2)	0.998	0.0011(2)
W	4e	0.2397(2)	0.9804(3)	0.0271(2)	0.002	0.0011(2)
O1	4e	0.115(1)	0.204(1)	0.213(1)	1.000	0.0032(4)
O2	4e	0.405(1)	0.710(1)	0.306(1)	1.000	0.0032(4)

Table SIII: Microwave-synthesized $W_{0.086}V_{0.914}O_2$, *P4₂/mnm*, structural parameters: *a* = 4.5655(9) Å, *b* = 4.5655(9) Å, *c* = 2.87168(6) Å, $U_{22} = U_{11}$, $U_{13} = U_{23} = 0.0$ Å^2

Atom	Wyckoff Position	x	y	z	Occ.	U_{11} (Å^2)	U_{33} (Å^2)	U_{12} (Å^2)
V	4e	0.0	0.0	0.0	0.933(1)	0.0008(4)	0.0185(7)	0.0031(6)
W	4e	0.0	0.0	0.0	0.067(1)	0.0008(4)	0.0185(7)	0.0031(6)
O	4e	0.3011(4)	0.3011(4)	0.0	1.0	0.007(1)	0.014(1)	0.009(1)

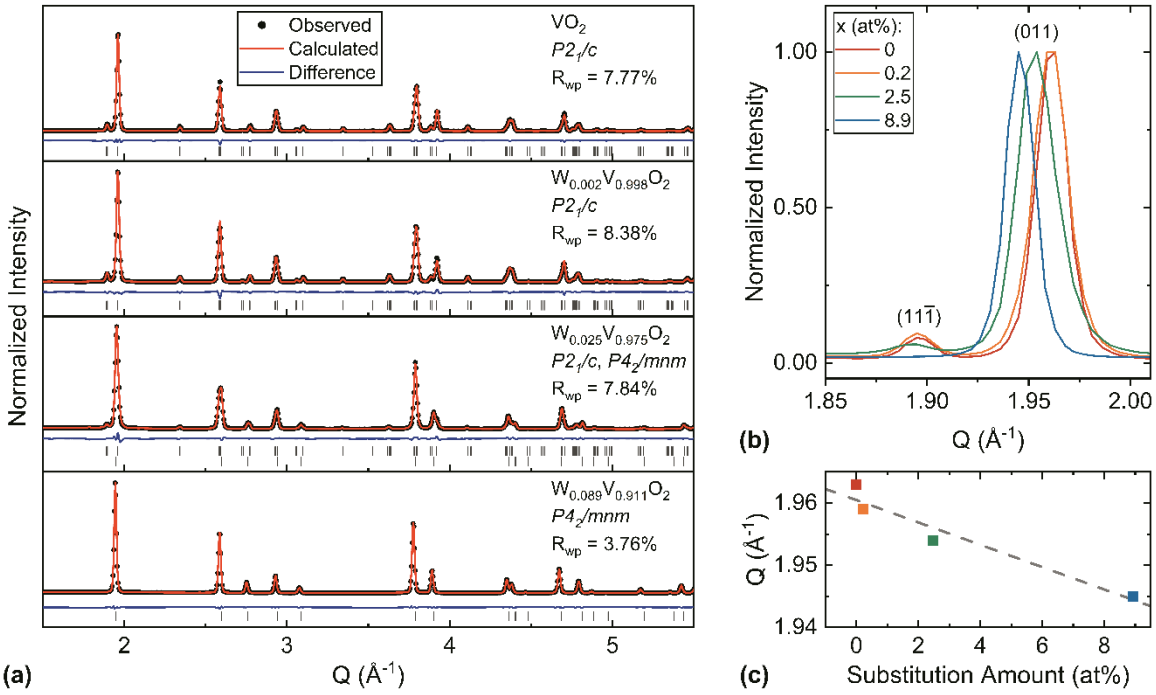

Figure S2: (a) Rietveld refinement for corresponding furnace-synthesized $W_xV_{1-x}O_2$ samples indicating similar phase purity to the microwave synthesized samples illustrated by the low fit residuals The phase associated with each fit is labeled on the top right corner of the plot and phase markers are in grey at the bottom of the respective plot. **(b)** Tracking the (011) peak shift as the structure symmetrizes with increasing substitution amount **(c)** Linear regression of the (011) peak centers as a function of substitution amount producing fit results: $Q = 1.960(2) - 0.0018(3)x$, $R^2 = 0.9333$

Table SIV: Furnace-synthesized VO_2, *P2₁/c*, structural parameters:
a = 5.752(3) Å, *b* = 4.5254(2) Å, *c* = 5.382(2), *b* = 122.610(4)°

Atom	Wyckoff Position	x	y	z	Occ.	U_{iso} (Å^2)
V	4e	0.2388(3)	0.9798(3)	0.0264(3)	1.0	0.0035(3)
O1	4e	0.104(1)	0.212(1)	0.205(1)	1.0	0.0064(4)
O2	4e	0.405(1)	0.707(1)	0.302(1)	1.0	0.0064(4)

Table SV: Furnace-synthesized $W_{0.002}V_{0.998}O_2$, *P2₁/c*, structural parameters:
a = 5.754(4) Å, *b* = 4.5269(3) Å, *c* = 5.382(4) Å, *b* = 122.593(7)

Atom	Wyckoff Position	x	y	z	Occ.	U_{iso} (Å^2)
V	4e	0.2389(3)	0.9810(4)	0.0269(4)	0.995(1)	0.0040(4)
W	4e	0.2389(3)	0.9810(4)	0.0269(4)	0.005(1)	0.0040(4)
O1	4e	0.105(2)	0.210(2)	0.205(2)	1.0	0.0068(6)
O2	4e	0.407(2)	0.708(2)	0.304(2)	1.0	0.0068(6)

Table SVI: Furnace-synthesized $W_{0.089}V_{0.911}O_2$, *P4₂/mnm*, structural parameters:
a = 4.56604(6) Å, *b* = 4.56604(6) Å, *c* = 2.86885(4) Å, $U_{22} = U_{11}$, $U_{13} = U_{23} = 0.0$ Å^2

Atom	Wyckoff Position	x	y	z	Occ.	U_{11} (Å^2)	U_{33} (Å^2)	U_{12} (Å^2)
V	4e	0.0	0.0	0.0	0.911(1)	0.0077(3)	0.0109(4)	0.0013(4)
W	4e	0.0	0.0	0.0	0.089(1)	0.0077(3)	0.0109(4)	0.0013(4)
O	4e	0.2994(2)	0.2994(2)	0.0	1.0	0.0012(6)	0.0047(9)	0.0006(7)

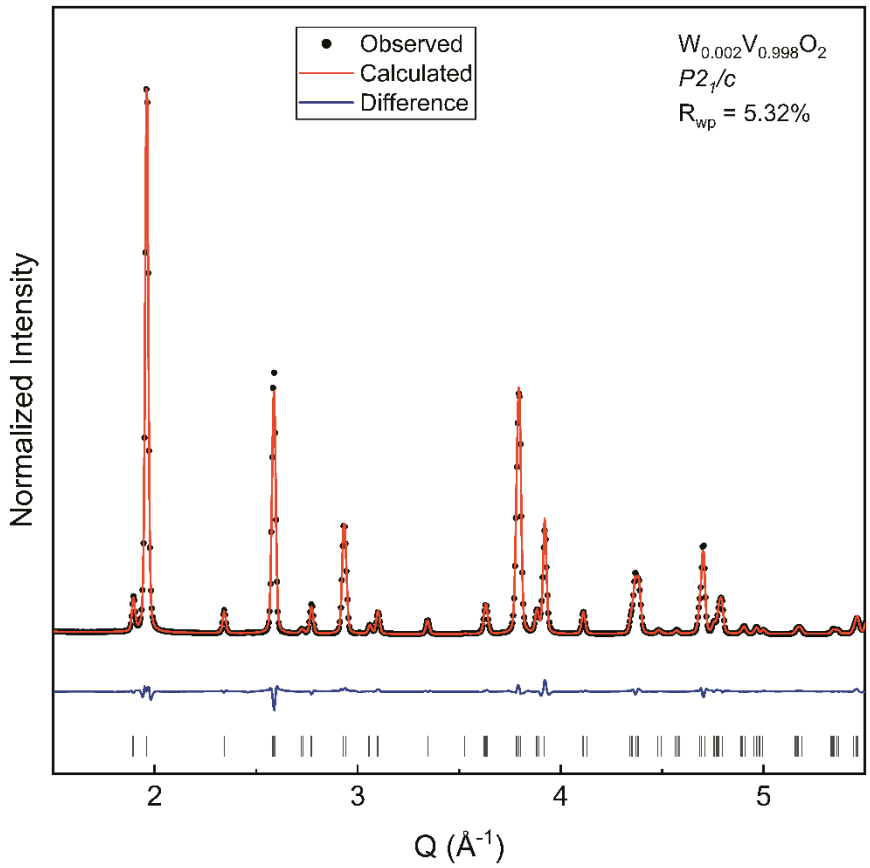

Figure S3: Rietveld refinements (l = 0.2399 Å) of DSC sample indicating similar phase purity as the samples presented in the main text

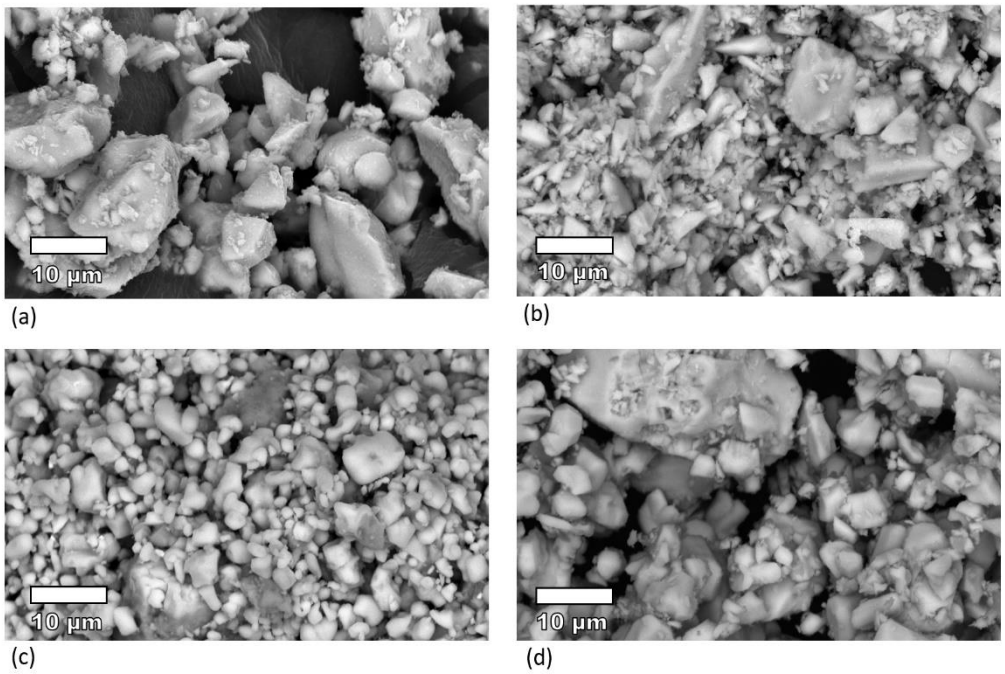

Figure S4: SEM Images of **(a)** VO_2 microwave, **(b)** VO_2 furnace, **(c)** $W_{0.80}V_{0.92}O_2$ microwave, **(d)** $W_{0.10}V_{0.90}O_2$ furnace (nominal substitution amounts).

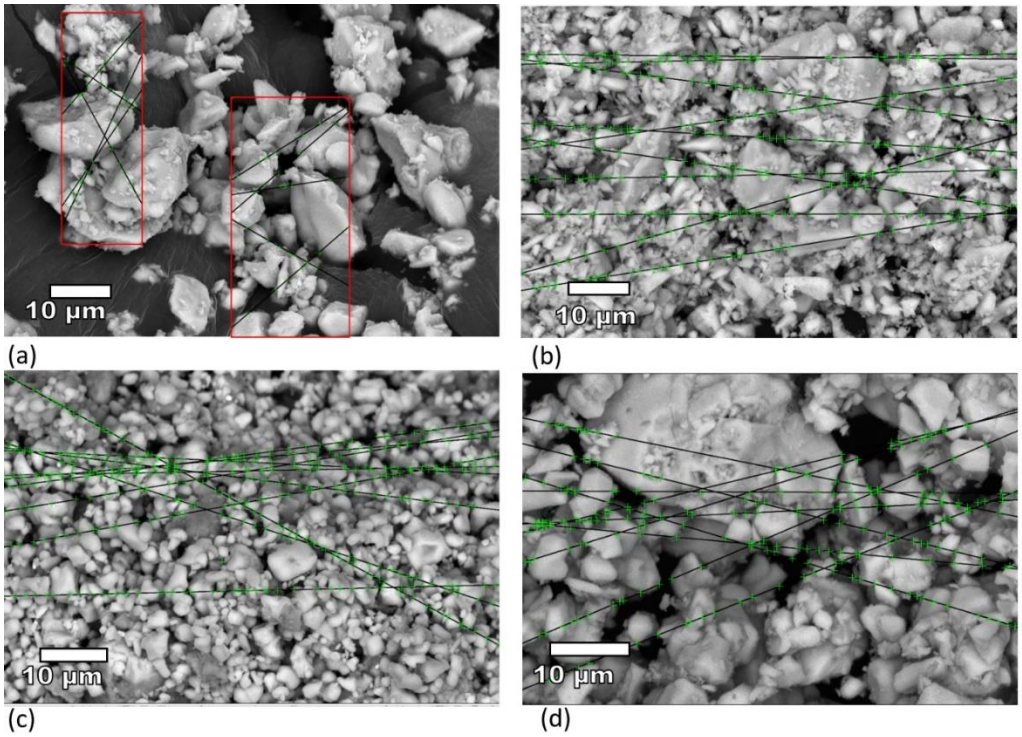

Figure S5: SEM images with overlaid lines and intercept crosshairs used to calculate grain size for **(a)** VO_2 microwave, **(b)** VO_2 furnace, **(c)** $W_{0.80}V_{0.92}O_2$ microwave, **(d)** $W_{0.10}V_{0.90}O_2$ furnace (nominal substitution amounts).

Table SVII: Grain size results for the SEM images shown in Figure S7

Nominal at% W	Synthesis	Mean Intercept Length	Average Grain Size
0	Microwave	3.12 μm	5.54 μm
0	Furnace	2.29 μm	4.06 μm
8	Microwave	1.83 μm	3.25 μm
10	Furnace	2.79 μm	4.95 μm

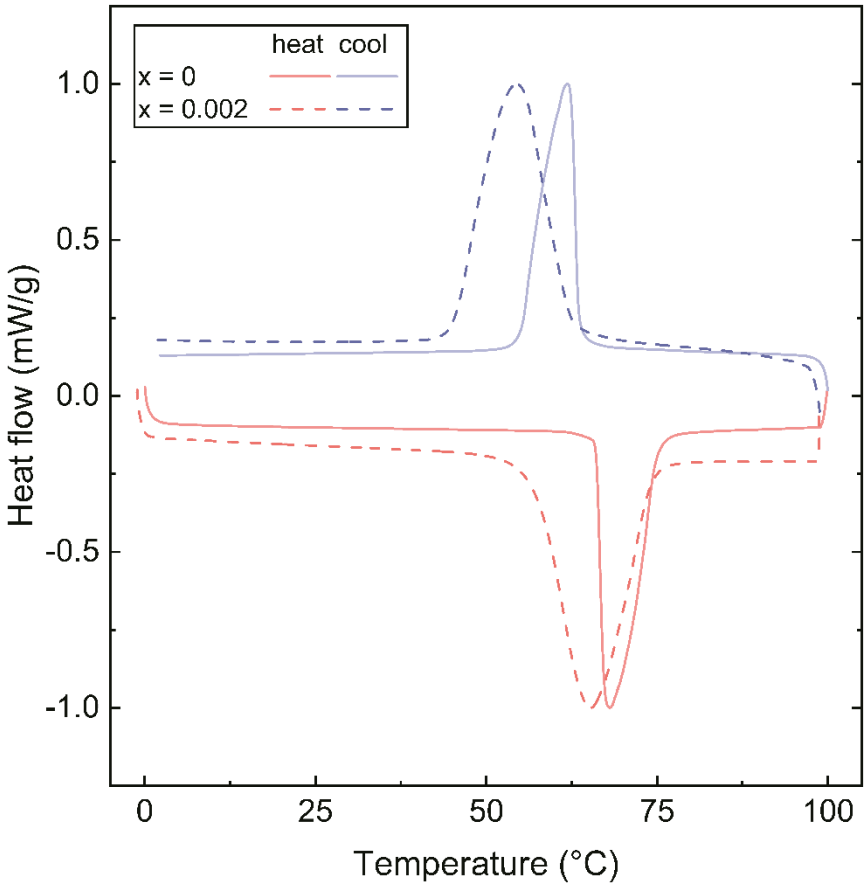

Figure S6: DSC data for microwave-synthesized $W_xV_{1-x}O_2$ of similar composition to those presented in the main text illustrating similar Tc's compared to SQUID data; however, 4.4 at% has two Tc's corresponding to W-rich and W-deficient areas within the sample

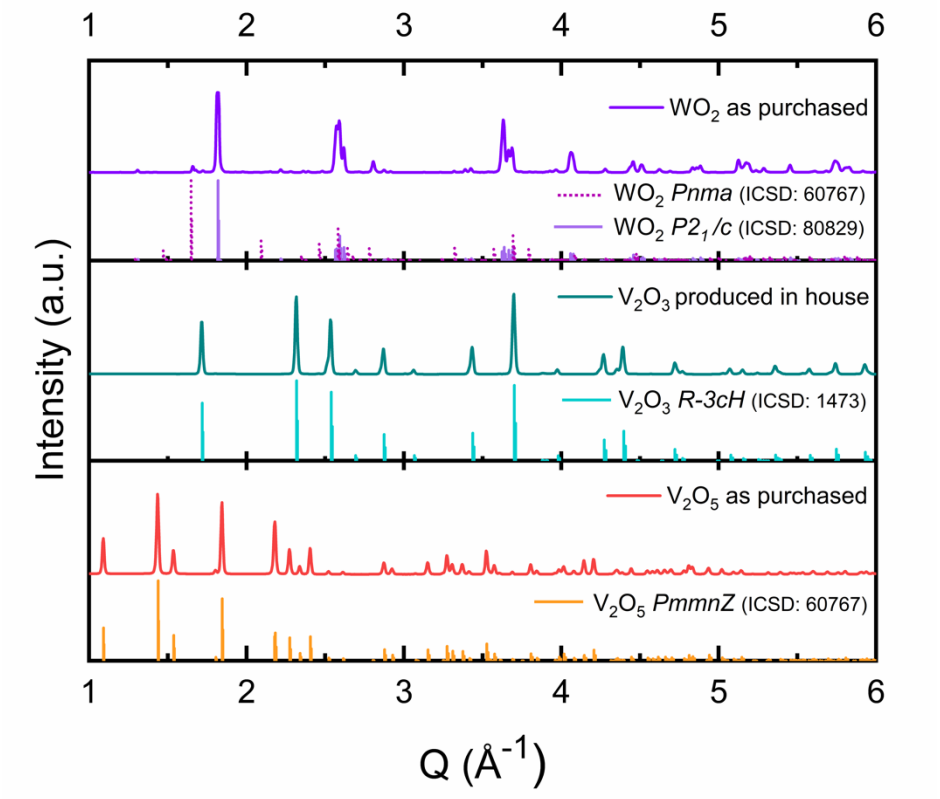

Figure S7: Phase purity of the precursors confirmed with XRD (λ=0.24162). As purchased WO_2 has a slight *Pnma* impurity

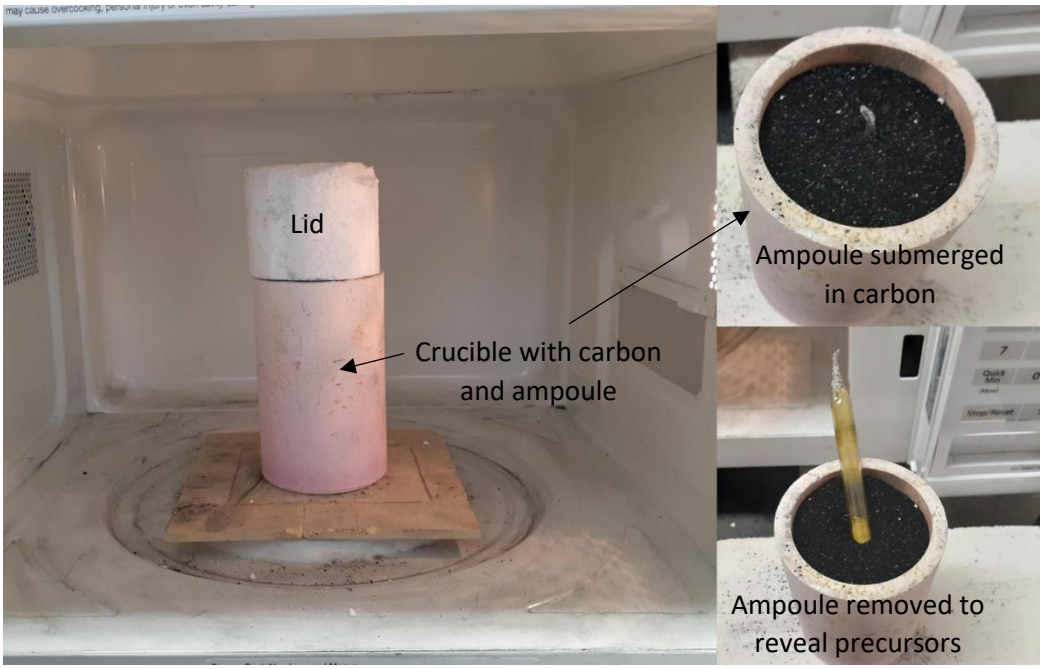

Figure S8: Experimental set up for microwave heating

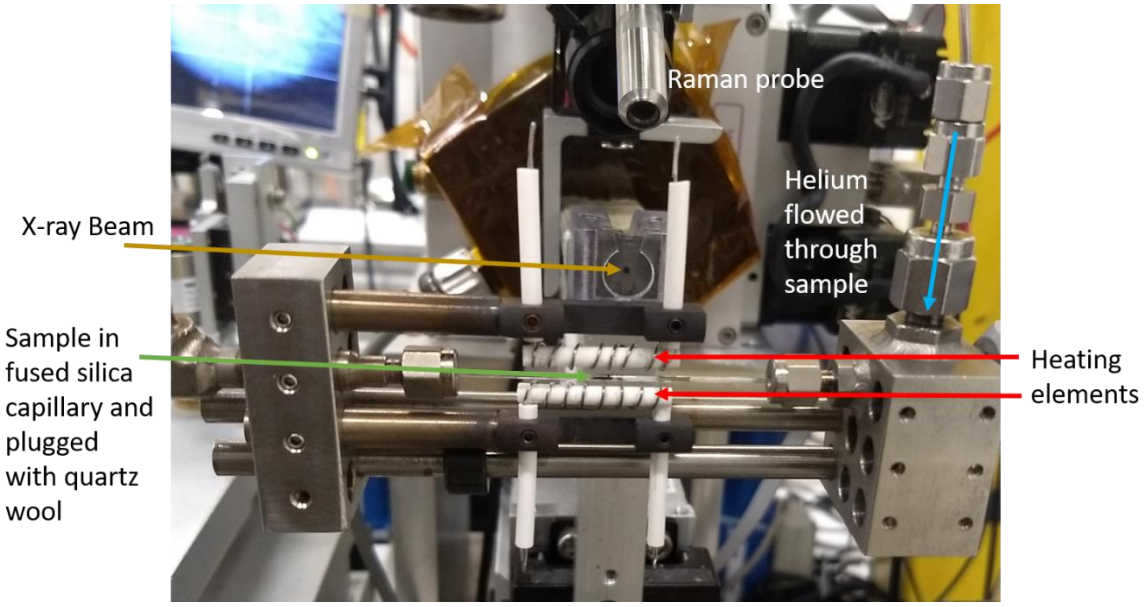

Figure S9: *In-situ* XRD experimental set-up with furnace performed at beamline 17-BM at the APS at ANL